WELDING RESEARCH

SUPPLEMENT TO THE WELDING JOURNAL, JANUARY, 1983

Sponsored by the American Welding Society and the Welding Research Council

RESEARCH/DEVELOPMENT/RESEARCH/DEVELOPMENT/RESEARCH/DEVELOPMENT/RESEARCH/DEVELOPMENT/RESEARCH/DEVELOPMENT/RESEARCH/DEVELOPMENT

An Investigation of Heat-Affected Zone Hot Cracking in Alloy 800

The susceptibility to grain boundary liquation in the HAZ is associated with localized titanium enrichment

BY J. C. LIPPOLD

ABSTRACT. The heat-affected zone (HAZ) hot cracking susceptibility of alloy 800 was evaluated using the Spot Varestraint test. Hot cracks were localized at liquated HAZ grain boundaries adjacent to the fusion line. Microprobe analysis of the liquated, crack-susceptible boundaries revealed a 50-fold increase in titanium concentration relative to the bulk composition. A Ti-rich Laves phase, which exhibits a melting point approximately 50°C (122°F) below the bulk solidus temperature, was associated with the liquated boundary region.

A mechanism involving the dissolution of Ti-rich carbides and assimilation of the titanium into migrating HAZ grain boundaries has been proposed to explain the HAZ hot cracking phenomenon. Both the nature and distribution of carbides (or carbonitrides) in the base metal microstructure were found to have a profound effect on the hot cracking behavior of alloy 800.

Introduction

Alloy 800 is a fully austenitic Fe-Cr-Ni alloy (also commonly known as Incoloy 800) often used in applications that require a combination of high-temperature strength and corrosion resistance. The alloy has been used extensively by the nuclear power industry for superheater and reheater tubes and, more recently, has been chosen by the solar energy industry for solar central receiver panels in multi-kilowatt power plants. Since all of these applications require welding as a fabrication step, alloy 800 must be resistant to hot cracking during welding and ultimately must exhibit as-welded properties that will ensure extended service life in severe mechanical/environmental conditions.

Although fusion zone hot cracking in alloy 800 can usually be avoided by the selection of appropriate filler materials, hot cracking in the heat-affected zone (HAZ) of certain heats of material has become a persistent and, as yet, unexplained phenomenon. An initial investigation by Canonico, et al., (Ref. 1) evaluated the effect of aluminum, titanium, sulfur, and phosphorus on the hot ductility behavior of Gleeble-simulated HAZ microstructures. Their results indicated that ductility losses were associated with an increase in each of these elements relative to a baseline Fe-Cr-Ni ternary composition. The elevated temperature embrittlement occurred abruptly at temperatures slightly below the solidus temperature and was intergranular in nature. The premature loss of ductility was associated with the formation of low-melting grain boundary films. However, no mechanism was proposed which would either explain the liquation phenomenon or rationalize the hot cracking sensitivity in the HAZ of isolated heats of alloy 800.

In another report, Reed and King (Ref. 2) found that the susceptibility to HAZ hot cracking as determined by the Spot Varestraint test was related to the elemental ratio (Al + Ti)/(C + Si). This ratio had been suggested earlier by York and Flury (Ref. 3) as a means to predict the hot cracking susceptibility of autogenous EB welds in alloy 800. York and Flury found that as the value of this ratio increased the alloy was less susceptible to cracking within the fusion zone. It is unclear how this ratio pertains to the behavior of the HAZ especially since Canonico, et al., (Ref. 1) demonstrated that an increase in titanium and aluminum promoted embrittlement in simulated HAZ hot ductility samples.

This investigation attempts both to identify the elemental species responsible for HAZ hot cracking in commercial heats of alloy 800 and to propose a model which describes the mechanics of the hot cracking phenomenon.

Experimental Procedure

Material

Five commercial heats of alloy 800 were evaluated in this investigation. The compositions of these materials are listed in Table 1. Heats B through E were supplied in bar stock form, while heat A was in the form of 6.35 mm (0.25 in.) thick plate. Heats A, B, D, and E were mill annealed at 980°C (1860°F) and heat C was solution annealed at 1150°C (2100°F).

The resultant microstructures are shown in Fig. 1. The mill annealing treatment results in a small grain size (ASTM 8-10) and a bimodal distribution of carbides. Annealing at 1150°C (2100°F) results in the dissolution of the smaller carbides and a subsequent increase in grain size (ASTM 3-5) as evidenced by the microstructure of heat C in Fig. 1.

Based on paper presented at the 62nd Annual AWS Meeting held in Cleveland, Ohio, during April 5-10, 1981.

J. C. LIPPOLD is a member of the Technical Staff at Sandia National Laboratories, Livermore, California.

Table 1—Alloy 800 Chemical Composition, Wt-%[(a)]

Heat identification	C	Mn	Si	Ti	Al	Cu	Cr	Ni	S	P	N	Fe
A (HH 7055A)	0.06	0.87	0.39	0.42	0.19	0.64	19.94	33.95	0.003	<0.01	0.020	Bal.
B (HH 8579A)	0.08	0.93	0.08	0.49	0.40	0.71	19.55	32.47	0.004	0.008	0.018	Bal.
C (HH 8144A)	0.04	0.87	0.24	0.43	0.39	0.57	19.67	32.79	0.004	0.007	0.012	Bal.
D (HH 8989A)	0.05	0.63	0.26	0.42	0.30	0.67	19.88	31.88	0.004	0.008	0.019	Bal.
E (HH 9019A)	0.07	0.81	0.15	0.44	0.47	0.32	20.42	32.83	0.003	0.008	0.017	Bal.

(a) Average of two independent analyses.

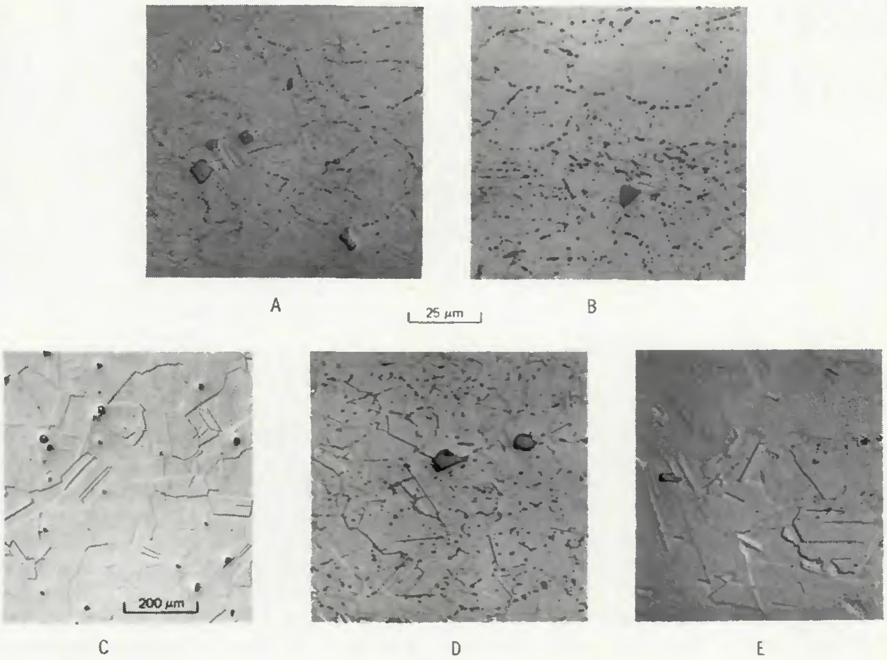

Fig. 1—Microstructure of the as-received base materials. Heats A, B, D, and E are in the mill annealed condition, X800. Heat C is in the solution-annealed condition, X100

Varestraint Testing

The Spot Varestraint test (Ref. 4, 5) was employed to evaluate the HAZ hot cracking susceptibility of the five base materials. A schematic illustration of the Spot Varestraint apparatus is shown in Fig. 2 (Ref. 6). Small laboratory scale samples 15.24 × 2.54 × 0.64 cm (6.0 × 1.0 × 0.25 in.) are clamped into the test fixture as indicated in the schematic. A gas tungsten arc (GTA) spot weld is initiated and after a predetermined time a pneumatically actuated ram is triggered, forcing the sample to conform to the radius of a preselected die block.

The welding parameters employed in the test are listed in Table 2. An arc time of 10 seconds(s) was selected in order to ensure that the specimen reached thermal equilibrium prior to testing. A delay time between arc shutoff and ram actuation was used to allow some solidification of the weld pool to occur prior to bending. Using this method cracks are produced in the HAZ adjacent to the fusion line of the GTA spot weld.

The tangential strain imparted to the outer fibers of the test bar is given by the relationship $\epsilon \approx t/2R$, where t is the thickness of the sample (6.4 mm, i.e., ¼ in.) and R is the radius of the die block. Augmented stains in the range from 0.25 to 4.0% were applied by selecting the appropriate die blocks.

Following testing, cracks in the HAZ were tabulated with the aid of a binocular microscope equipped with a filar eyepiece. A magnification of ×100 was used to measure crack lengths on the as-tested surface of the Varestraint samples. The crack length data reported represents the average of two independent compilations. The total crack length, maximum crack length, total number of cracks, and average crack length were used to assess the hot cracking susceptibility of the individual heats.

Microstructural Evaluation

Metallographic samples were prepared in order to investigate the microstructural features of the HAZ. All samples were polished through 0.05 µm alumina powder and etched with a solution containing equal parts of hydrochloric, sulfuric, and nitric acid. Pertinent regions of these samples were also evaluated using the scanning electron microscope (SEM) and the electron microprobe.

Table 2—Alloy 800 Spot Varestraint Welding Parameters

Current	150 ± 5 A
Voltage	14 ± 1 V, DCSP
Electrode-to-work distance	2.38 mm (3/32 in.)
Electrode	W-ThO$_2$, 60 deg included angle
Electrode diameter	2.38 mm (3/32 in.)
Arc time	10 s
Ram delay time	0.05 s
Shielding gas	Argon
Flow rate	0.23 liters/s (30 cfh)

Several samples were partially sectioned and then fractured at room temperature in order to expose the fracture surfaces of the HAZ cracks. The crack surface morphology was evaluated in the SEM. Both the surface concentrations and composition depth profiles below the crack surfaces were analyzed with aid of the scanning Auger microscope.

Results

Base Metal Microstructure

Polished and etched metallographic samples of the as-received material were examined in the SEM in order to determine the nature of the base metal carbides. An SEM micrograph of the heat A microstructure, which is representative of a mill annealing heat treatment at 980°C (1800°F), is shown in Fig. 3. The microstructure consists of a bimodal distribution of carbides (or carbonitrides) with large, blocky MC-type particles located randomly throughout the structure and smaller MC and $M_{23}C_6$ particles outlining prior austenite grain boundaries.

The large MC carbides were found to be Ti-rich and presumed to have formed in the melt prior to solidification of the original ingot. The smaller MC particles which were also rich in titanium and the $M_{23}C_6$ particles which were enriched in chromium form during the mill annealing heat treatment. In a report by Allen and Jones (Ref. 7), thin foil TEM samples from heats B, D, and E were prepared and diffraction patterns of the individual particles were produced which verified the

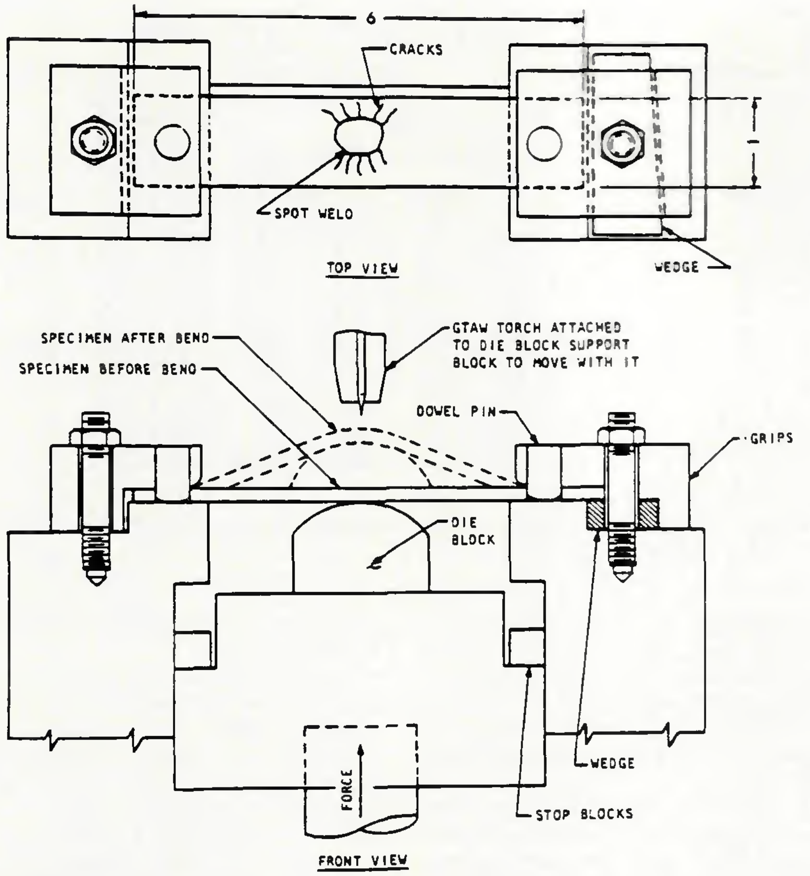

Fig. 2 — Schematic of the Spot Varestraint apparatus (Ref. 6)

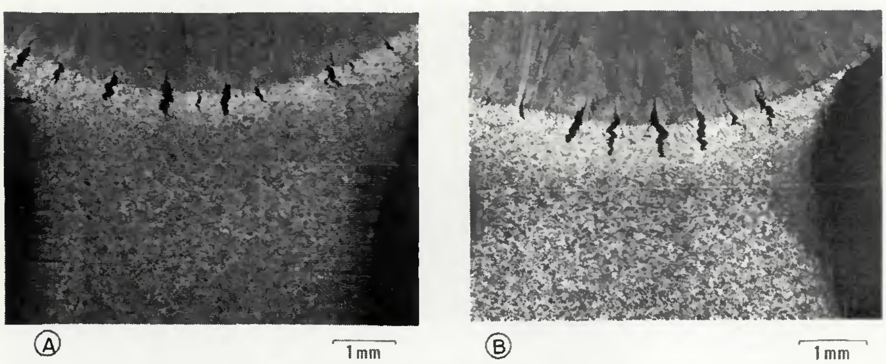

Fig. 4 — Macrostructure of Spot Varestraint specimens tested at 4% restraint: A — heat B; B — heat D. X30 (reduced 42%, on reproduction)

nature of these particles.

The microstructure shown in Fig. 3 is typical of the mill annealed condition of heats A, B, D, and E. Heat C exhibited only large, blocky MC-type carbides typical of the solution annealed condition.

Spot Varestraint Results

The microstructure of both a heat B and heat D Spot Varestraint sample tested at 4% restraint is shown in Fig. 4. The light-etching annular region adjacent to the fusion line delineates the region of the HAZ where substantial grain growth has occurred during the test. Note that the cracks lie perpendicular to the fusion line and within the light-etching region.

In many cases the cracks extend into the fusion zone. Since a short delay occurs between the time the arc is extinguished and the sample is bent around the radius block, a small portion of the fusion zone solidifies prior to being subjected to the tangential stress. The portion of the fusion zone in which the cracks propagate corresponds to this pre-solidified region.

Crack Length vs. Augmented Strain. The relative hot cracking susceptibility of the individual heats of alloy 800 was evaluated by plotting the total length of all cracks observed on an individual sample vs. the strain level at which that sample was tested. The results of the Spot Varestraint test, plotted in this manner, are shown in Fig. 5. Although the individual curves fall within a broad band, the data suggest that both heats D and E are more susceptible to HAZ hot cracking than the other heats, particularly at the higher strain levels.

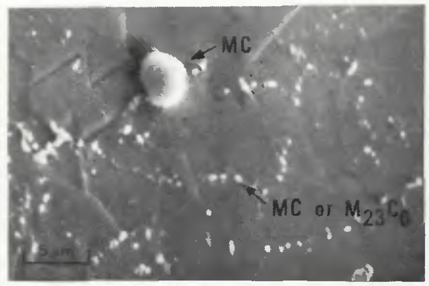

Fig. 3 — SEM micrograph of base metal carbides, X3000 (reduced 50%, on reproduction)

Samples of heat A material were tested in orientations both transverse (A-T) and parallel (A-L) to the rolling direction. Despite the difference in orientation there appears to be almost no change in hot cracking susceptibility when the direction of crack propagation is parallel to the rolling direction.

Differences in the hot cracking behavior of the five heats can be made clearer if both the cumulative total crack length and total number of cracks from the data in Fig. 5 are plotted in the form of a bar graph, as shown in Fig. 6. When the data are plotted in this manner it can be seen that heat A, tested in the transverse orientation, and heat C are least susceptible to HAZ hot cracking. Heats D and E exhibit nearly a 50% increase in cumulative total crack length and total number of cracks relative to heats A and C.

Microstructural Evaluation

Metallographic sections parallel to the top surface of the test samples were examined at higher magnification. This was done in order to determine the metallurgical changes which have occurred in the HAZ as a result of the Spot Varestraint test and to relate the onset of hot cracking to microstructural features in this region.

Polished and etched sections of the HAZ containing hot cracks in heats A, C, and E are shown in Fig. 7. All the cracks propagate intergranularly along boundaries in the grain coarsened region of the HAZ. Continuity of the fracture path across the fusion line into the fusion zone is a consequence of the epitaxial nature of solidification in fusion welds, whereby grain boundaries are continuous across the fusion line.

Closer inspection of the microstructure in the crack-susceptible grain coarsened region reveals that localized melting has occurred along many of the grain boundaries. A region of the HAZ in a heat A sample tested at 4% restraint is shown in Fig. 8. Note the widened boundaries (arrows) associated both with grain

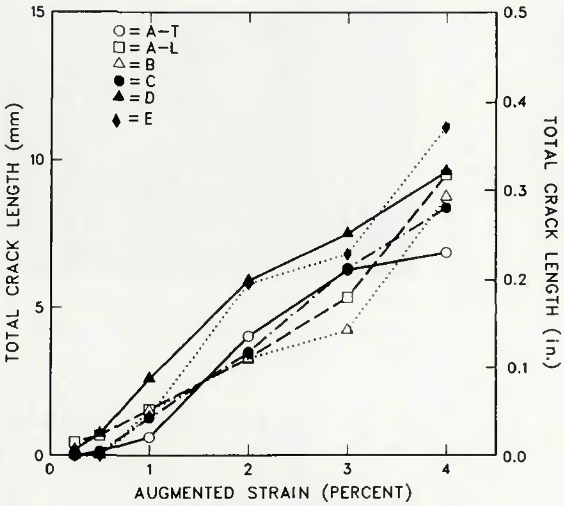

Fig. 5 — Results of the Spot Varestraint test plotted as total crack length vs. augmented strain

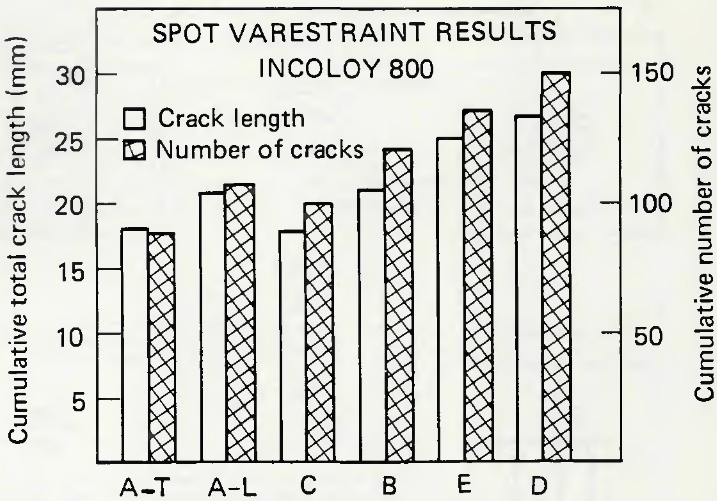

Fig. 6 — Cumulative total crack length and cumulative number of cracks for five heats of alloy 800

Fig. 7 — Regions of hot cracking in the HAZ of samples tested at 4% restraint: A — heat A-T; B — heat C; C — heat E ×100

boundaries along which fracture has occurred and with boundaries which have remained intact. The widened boundaries are indicative of the localized melting and resolidification which has occurred at these sites during the Varestraint Test.

A secondary constituent was often observed along the center of the melted and resolidified grain boundary regions. This dark etching constituent, shown more clearly in the inset in Fig. 8, appears to be nearly continuous and forms along solidification substructure boundaries within the perimeter of the liquated region. The presence of this secondary constituent along the subboundaries indicates that it formed during the final stages of resolidification.

Microprobe Results. Electron beam microanalysis was performed at selected locations within the crack-sensitive HAZ microstructure. The microprobe results from a heat A sample tested at 4% restraint are presented in Fig. 9. Two points (A and C) along the widened grain boundaries and two reference points (B and D) at the grain interiors were analyzed. The compositional data in Fig. 9 represent an average of three individual analyses at each point.

A comparison of the local composition along the boundaries with both the adjacent HAZ composition and the nominal

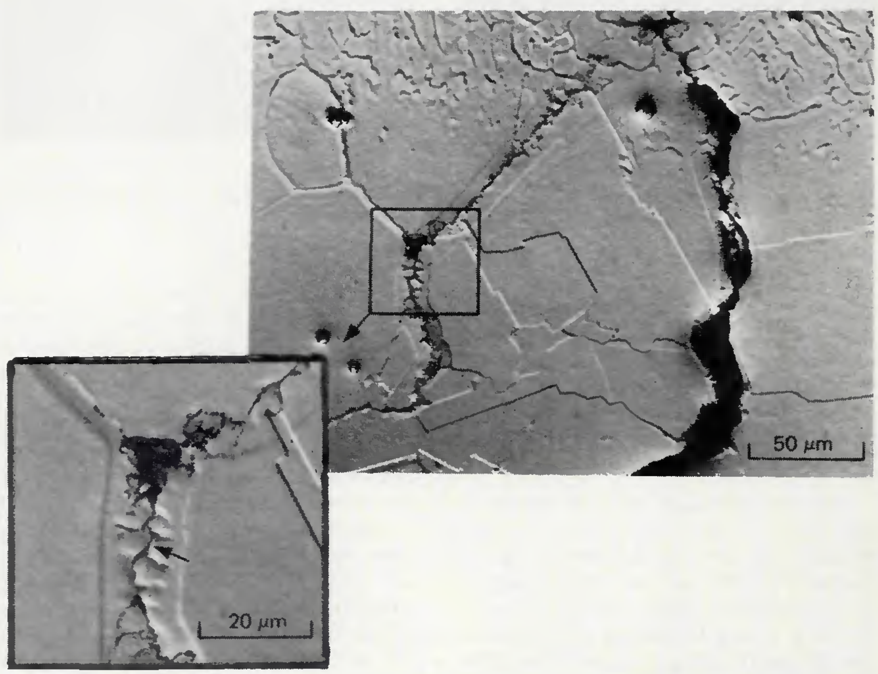

Fig. 8 — Grain boundary liquation associated with HAZ hot cracks in a heat A sample tested at 4% restraint, ×400. Note the secondary constituent along the liquated boundary in the inset, ×1000 (×400 and ×1000 views reduced 7% on reproduction)

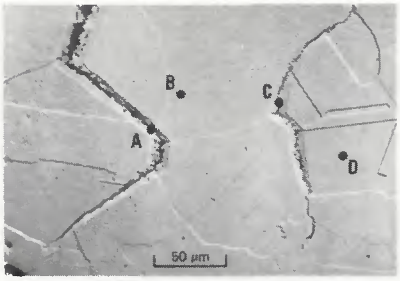

Microprobe Results (wt.%)

	A	B	C	D	Nominal
Ti	18.56	0.28	18.19	0.26	0.42
Si	0.81	0.55	1.30	0.57	0.39
Al	0.22	0.11	0.22	0.15	0.19
Mn	1.46	1.01	0.99	1.00	0.88
Mo	0.40	0.21	0.24	0.19	<0.05
Cu	0.91	0.65	0.95	0.14	0.64
Cr	22.70	20.64	23.68	19.83	19.94
Ni	35.57	34.46	36.35	33.06	33.95
S	<0.01	<0.01	<0.01	<0.01	0.003
P	1.03	0.01	1.71	0.01	<0.01
C	-	-	0.16	-	0.06
Fe*	18.33	42.07	16.20	44.78	43.47

*determined by difference

Fig. 9—Microprobe analysis results of selected regions of the HAZ of a heat A sample tested at 4% restraint, ×400 (reduced 16% on reproduction)

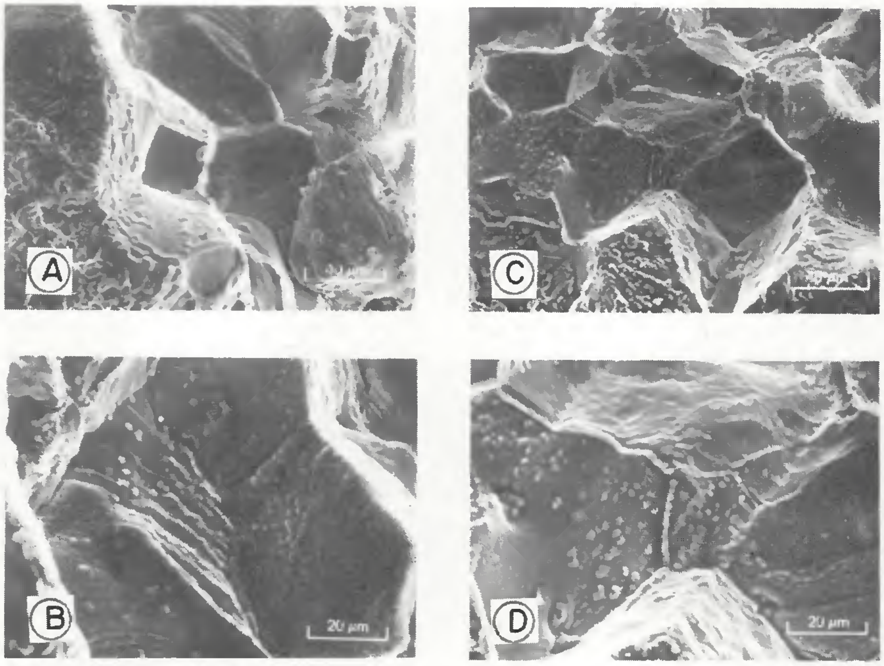

Fig. 11—Fractography of HAZ crack surfaces of Spot Varestraint samples tested at 4% restraint; A—heat A-T, ×500; B—heat A-T, ×1000; C—heat D, ×500; D—heat D, ×1000

alloy composition indicates that a significant enrichment of titanium and phosphorus occurs at points A and C. There also appears to be a slight increase in silicon, copper, chromium, and carbon along the melted and resolidified boundaries. Sulfur was not detected at any of the analysis points. Microprobe analysis of liquated boundaries and in the heat C and E samples yielded similar results; in both cases a significant enrichment in titanium was observed along HAZ grain boundaries.

Temperature Gradient in the HAZ

One sample was thermally monitored during the Spot Varestraint test by imbedding thermocouples in the HAZ at various distances from the fusion line. The temperatures at the individual locations were measured simultaneously during the test cycle. The thermal data indicated that, for the welding parameters and the specimen geometry employed, the system reaches nearly steady-state thermal equilibrium in 10 s.

The steady-state temperature gradient in the near HAZ region at the instant that the specimen is bent in the test sequence is shown in Fig. 10. Superimposed on this temperature vs. distance plot is the corresponding microstructure in the HAZ of a heat B test specimen. A distinct temperature regime can be identified in which grain boundary liquation and subsequent

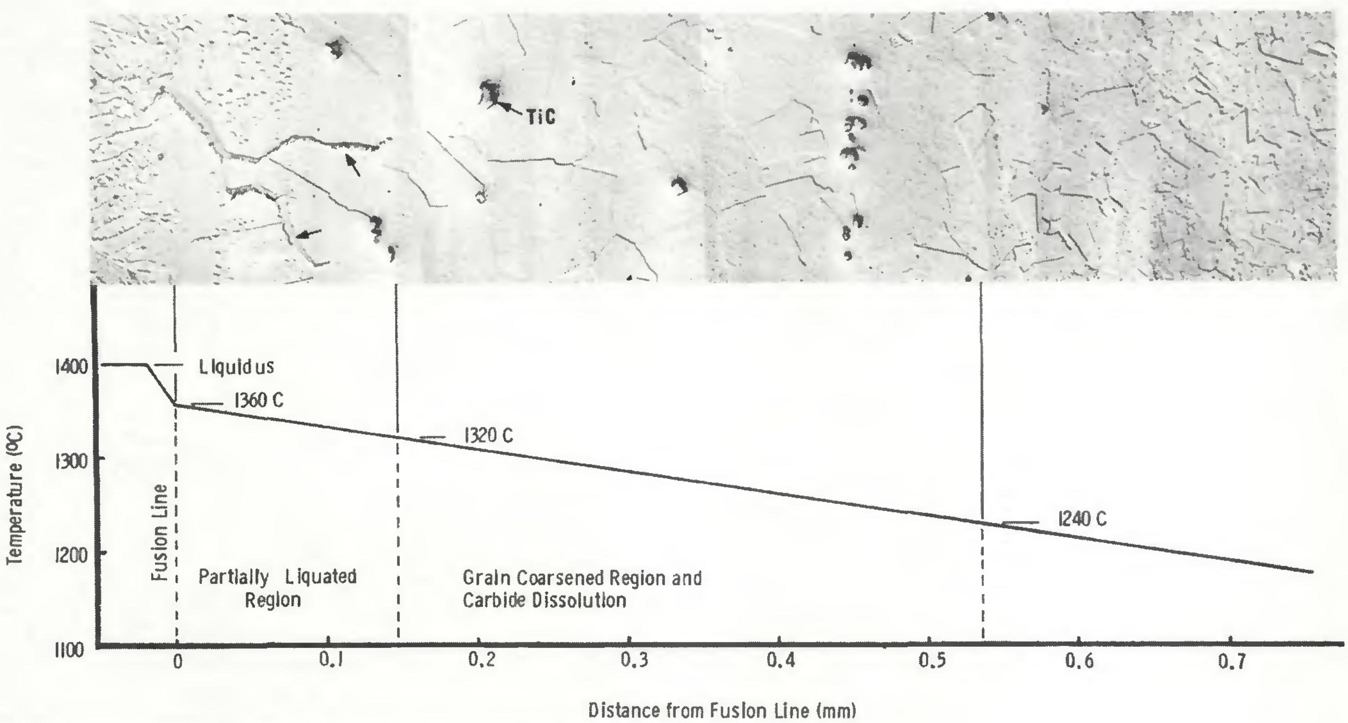

Fig. 10—Temperature gradient in the HAZ of an alloy 800 Varestraint sample

hot cracking occurs; this is accomplished by measuring the distance from the fusion line to the furthest indication of grain boundary melting and relating this distance to the measured temperature gradient. In this way it can be shown that grain boundary melting occurs in the temperature range from 1360 to 1320°C (2480 to 2410°F).

Further from the fusion line, a grain coarsened region forms in the temperature range from 1320 to 1240°C (2410 to 2265°F). The rapid transition in grain size, which occurs at approximately 1240°C (2265°F), represents the point at which carbides dissolve and thus become ineffective in pinning the grain boundaries. Note that the large, blocky Ti-rich carbides do not dissolve as readily as the smaller MC and $M_{23}C_6$ particles in both the partially liquated region and the grain coarsened region.

Analysis of Fracture Surfaces

Heat A and E Varestraint specimens were sectioned in order to reveal the HAZ hot crack fracture surfaces. The morphology of a region of the fracture surface near the fusion line, shown in Fig. 11, reveals the intergranular nature of the crack path. Careful examination of the fracture surfaces revealed a wavy pattern on the grain faces and evidence of melting along grain boundaries and at triple points. Both observations suggest that failure has occurred by a liquation mechanism rather than by a solid-state failure mode which would produce a smoother intergranular fracture morphology.

The fracture surfaces also exhibit a distinct speckled appearance at regions adjacent to, but not within, the fusion zone. The density of these speckles decreases as a function of distance from the fusion line. The origin of these discrete regions may be merely a by-product of the fracture mechanism, whereby the speckles represent the last vestiges of liquid which bridged the boundary prior to complete separation.

Upon separation, the microscopic liquid droplets resolidified as the discrete particles observed in Fig. 11. Alternatively, these distinct particles may represent the dark-etching constituents observed along the fracture path in Fig. 8 or may form by means of a precipitation mechanism as the weld cools through the carbide precipitation range.

Auger Surface Analysis. The fracture surfaces were also subjected to analysis in the scanning Auger microscope. Since cracking along these grain boundaries occurs at elevated temperature, the fracture surface will be oxidized upon cooling to room temperature. As a result, it was necessary to ion-sputter through the surface in order to obtain information below the oxidized surface layer. Using this technique it was possible to obtain the compositional depth profiles for the heats A and D fracture surfaces presented in Fig. 12.

In both cases silicon and titanium are present at high levels on the surface, while the nickel, chromium, and iron concentrations are essentially zero. The oxygen and carbon curves have been deleted for clarity; however, it should be noted that oxygen which was initially high at the surface was nearly absent 100 Å below the surface. Silicon also decreases rapidly in the oxide layer but is still present in significant proportions below this level.

In both samples, titanium increased sharply and reached a maximum approximately 100 Å below the surface. Note that heat D, which was more susceptible to HAZ hot cracking than heat A, exhibits a higher concentration of titanium in the near-surface region. The Auger results also tend to corroborate the microprobe data (Fig. 9) which showed enrichment of both silicon and titanium along liquated grain boundaries. The Auger analysis failed to reveal the phosphorus enrichment which was detected by the microprobe.

Discussion

The results of the metallographic inspection, microprobe analysis, and Auger surface analysis have shown that cracking in the HAZ of alloy 800 weldments occurs preferentially at intergranular sites and involves localized melting associated with an enrichment in titanium and silicon. The dramatic increase in titanium concentration in these liquated regions (nearly a 50-fold increase over the nominal alloy concentration) requires a rapid reapportionment of titanium in the near-HAZ during the weld thermal cycle. The mechanism by which this reapportionment occurs and the relationship between titanium enrichment and the observed HAZ hot cracking is discussed in the following sections.

Grain Boundary Liquation

Metallographic evidence has shown that the HAZ cracking in Spot Varestraint test samples is associated with widened liquated boundaries adjacent to the fusion line. It has also been shown that in many cases the cracks are continuous across the fusion line into the fusion zone (Fig. 4), suggesting that fracture may occur initially in the fusion zone and that the widened HAZ grain boundaries may be the result of a crack backfilling mechanism.

The mechanism, as originally described by Savage and coworkers (Ref. 9), involves the backfilling of either HAZ or fusion zone cracks by liquid from the molten weld pool. As a crack forms at the solid-liquid interface, liquid is drawn into the open crack by capillary action where it solidifies within the confines of the crack envelope. As a result, the actual mechanism of HAZ cracking may be masked by the presence of backfilled liquid from the fusion zone.

In an effort to determine if the liquated boundary microstructure resulted primarily from a crack backfilling mechanism,

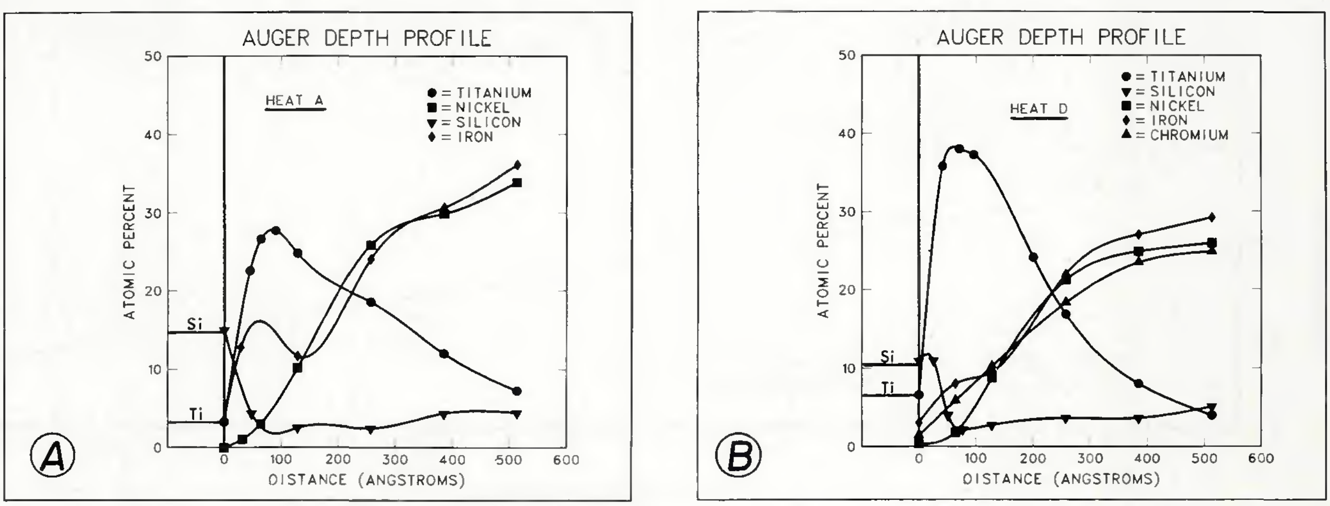

Fig. 12 — Compositional depth profiles of HAZ fracture surfaces obtained with the scanning Auger microscope: A — heat A; B — heat D

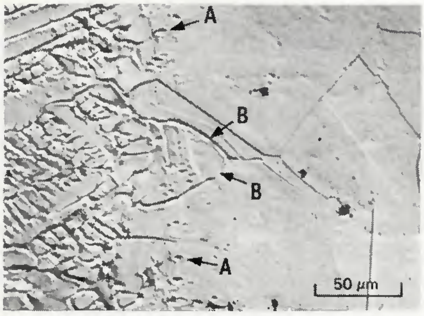

Fig. 13 — Microstructure in the near-HAZ of an unbent spot Varestraint sample. Note the constitutional liquation of carbides (A) and the localized melting of grain boundaries (B). X400 (reduced 50% on reproduction)

samples were produced which experienced the same thermal histories as Spot Varestraint samples; however, they were not bent to induce cracking in the HAZ. The microstructure along the fusion line of such a sample is shown in Fig. 13.

The features of the microstructure in Fig. 13 are similar to those observed in the Varestraint samples, as evidenced by the constitutional liquation of MC or $M_{23}C_6$ particles adjacent to the fusion line (denoted by A in Fig. 13) and the presence of widened, liquated boundaries in the near-HAZ (denoted by B). Microprobe analysis of these boundary regions revealed a localized enrichment in titanium, although not to the degree reported in Fig. 9.

The onset of liquation along grain boundaries in alloy 800 was also corroborated by the results of a companion study which evaluated the hot ductility of simulated HAZ microstructures (Ref. 10). Results of the study showed that liquation and associated ductility losses occurred in the temperature range from 1325 to 1350°C (2415 to 2460°F) for all five heats. SEM analysis of the hot ductility samples tested in this temperature range revealed that fracture was intergranular and exhibited a morphology similar to the fracture surface of the Varestraint samples shown previously in Fig. 11. The brittle temperature range defined by the hot ductility test is in good agreement with the embrittlement range predicted from the temperature gradient/microstructure comparison made in Fig. 10.

From the observations discussed above, it can be concluded that grain boundary liquation in the HAZ can be isolated from fusion zone phenomena. Although some degree of crack backfilling may contribute to the total volume of in situ liquid in the HAZ boundaries, it is clear that both embrittlement and titanium enrichment can occur in the absence of any backfilling. It should be noted that the widened, liquated boundaries observed in Fig. 8 are not evident in the reference microstructure in Fig. 13. This discrepancy can be explained by the same capillarity argument used previously.

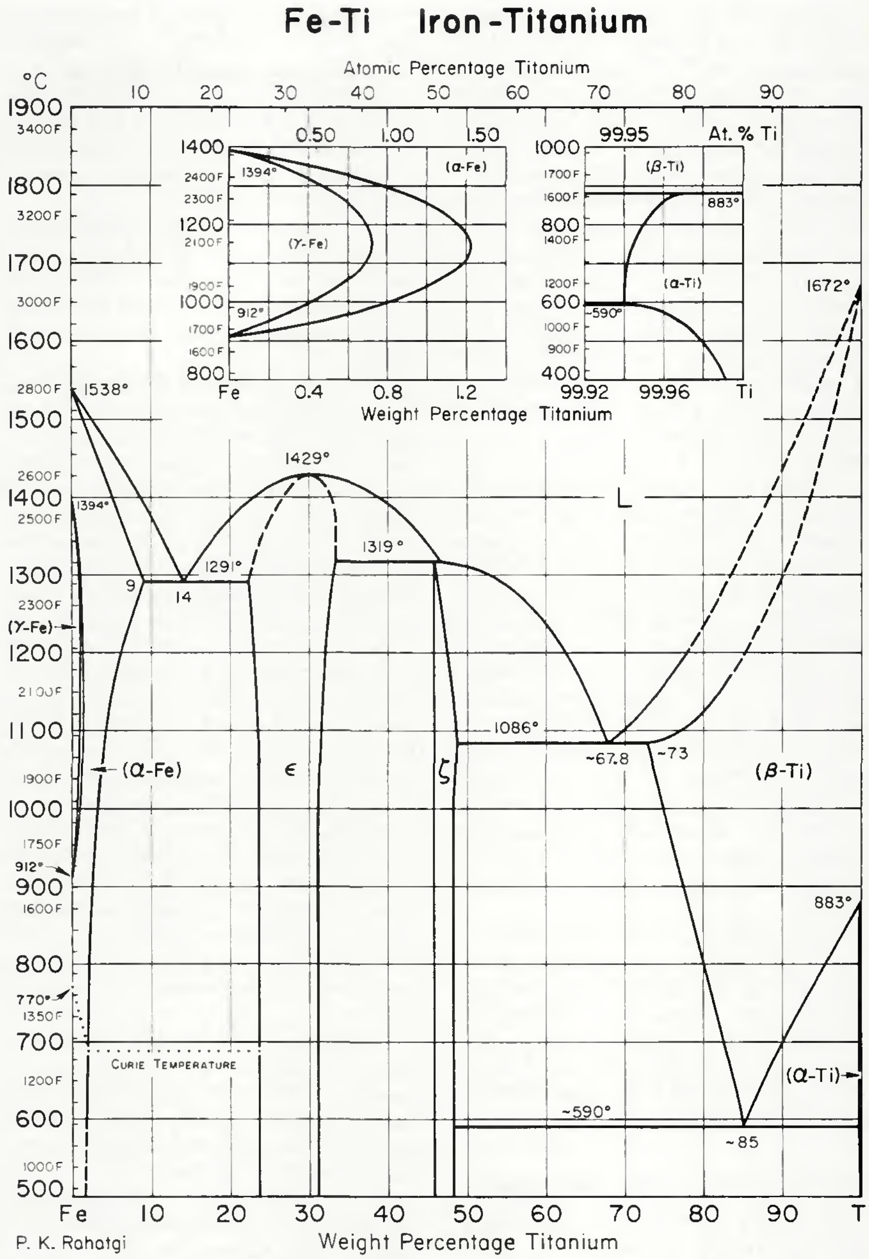

Fig. 14 — The Fe-Ti binary equilibrium diagram (Ref. 12)

If the sample in Fig. 13 was to be bent around a die block in the manner of the Spot Varestraint test, the boundaries at points B would separate in the presence of the tangential stress and the liquid along the boundary would be drawn into the root of the crack. As the crack propagated, the volume of liquid would increase until ultimately the stress field decreased and crack propagation ceased. The liquid would then solidify in situ and might result in widened boundaries similar to those shown in Fig. 8.

Nature of the Secondary Constituent

The presence of a secondary constituent along the center of the liquated HAZ boundaries suggests that this constituent is the last to form during the resolidification of the boundary region. Attempts to identify the constituent by means of extraction replication techniques were unsuccessful.

A similar constituent was observed by Brooks (Ref. 11) in a study of HAZ cracking in an A-286 stainless steel. Since the A-286 alloy nominally contains 15Cr-25Ni-2Ti, it is likely that the constituent may be similar to that found in the HAZ of alloy 800. The five-fold increase in the titanium content of A-286 relative to alloy 800 resulted in a larger volume of the constituent in the HAZ of A-286 test samples. Through the use of x-ray diffraction techniques Brooks (Ref. 11) was able to identify the constituent as a variant of the Fe_2Ti Laves phase.*

**Laves phase — a close packing of atoms involving two atoms of one metal and one atom of a second metal geometrically located in the matrix.*

Inspection of the Fe-Ti binary equilibrium phase diagram (Ref. 12) in Fig. 14 indicates that the Fe_2Ti phase forms via a eutectic reaction at 1291°C (2390°F). At the eutectic temperature the Fe_2Ti phase contains approximately 22 wt-% titanium. The composition predicted by the phase diagram is in good agreement with the microprobe analysis data of the liquated grain boundaries presented previously in Fig. 9 and corroborates the Auger surface analysis results in Fig. 12. In addition, the eutectic temperature of 1291°C (2390°F) correlates reasonably well with the onset of embrittlement observed in both the Spot Varestraint samples and in the hot ductility specimens ($\sim$ 1320°C, i.e., 2408°F).

It should be noted, as pointed out by Brooks (Ref. 11), that the actual phase is probably more complex than the simple Fe_2Ti stoichiometry. Substitution of other alloying elements, as in a more general M_2Ti phase, will have subtle effects on the phase equilibria, melting temperature, and quantity of the phase which forms. Although a lower temperature eutectic exists in the Fe-Ti system at Fe-67.8 Ti, there is no experimental evidence which indicates that this eutectic reaction is involved in the onset of HAZ hot cracking in alloy 800. For example, hot ductility samples tested at 1100°C (2012°F) showed no sign of embrittlement (Ref. 10).

The iron-silicon system also forms a eutectic at Fe-19Si at a temperature of $\sim$ 1200°C (2190°F). Segregation of silicon has been shown to promote hot cracking in other austenitic alloys and may contribute to the formation of low-melting films along grain boundaries in the HAZ of alloy 800.

Rationale for HAZ Grain Boundary Liquation

The results of microprobe and Auger analysis of HAZ grain boundaries in alloy 800 Spot Varestraint specimens have shown that the localized melting along these boundaries is most strongly associated with an enrichment in titanium. A large proportion of the titanium in the mill-annealed base metal microstructure is present in the form of discrete MC-type carbides. Consequently, it is evident that a rapid redistribution of titanium occurs in a narrow microstructural region adjacent to the fusion line during the duration of the test. Unfortunately, the rapid heating and cooling rates associated with the weld HAZ result in non-equilibrium microstructures, which are not easily rationalized by classical metallurgical principles.

Savage, et al., (Ref. 13, 14) have devised a "constitutional liquation" mechanism to explain the formation of liquid grain boundary films in the weld HAZ of maraging steel. Fundamentally, constitutional liquation involves the decomposition and subsequent melting of intermetallic particles in a region adjacent to the weld fusion line which is rapidly heated to near-solidus temperatures. As migrating grain boundaries intersect the liquated region at the particle-matrix interface, liquid penetrates the boundary and renders the microstructure susceptible to cracking.

Since its inception the constitutional liquation mechanism has been invoked by a number of investigators (Ref. 15-18) to account for the HAZ crack susceptibility of a variety of steel and nickel-base alloys.

There is evidence of constitutional liquation adjacent to the fusion line in alloy 800 — Figs. 9 and 12. Nonetheless, it appears that the localized melting of the Ti-rich carbides is not integrally involved in the grain boundary liquation mechanism. This observation is also supported by the metallographic evidence presented in Fig. 7. Note that liquated particles are restricted to a narrow band adjacent to the fusion line but are absent in the region of crack propagation in the portion of the HAZ further from the fusion line. This indicates that constitutional liquation of the carbides is restricted to a narrow temperature range slightly below the bulk solidus temperature; it also indicates that, at lower temperatures (see Fig. 9), the carbide particles dissolve in the matrix. Furthermore, there is no indication that the constitutional liquation of Ti-rich carbides serves to pin grain boundaries or otherwise promote the penetration of these boundaries by liquid films.

In the absence of a model based on the constitutional liquation theory, it appears that titanium enrichment of HAZ grain boundaries must depend on the interaction of matrix titanium and migrating boundaries as the HAZ is rapidly heated to near-solidus temperatures. The microstructural montage shown in Fig. 9 reveals that appreciable grain growth does not occur until the small MC and $M_{23}C_6$ carbides situated along prior austenite grain boundaries begin to dissolve. As a result an abrupt increase in grain size occurs in the temperature range above approximately 1240°C (2264°F).

Several investigators (Ref. 15, 19, 20) have suggested that, as the HAZ grain boundaries migrate, they "sweep up" solute and/or interstitial atoms from the matrix. The "sweeping" effect is most pronounced in the region adjacent to the fusion line where the diffusivity of the solute (or interstitial) atoms is high, allowing the atoms to diffuse with the moving grain boundary.

Owczarski, et al., (Ref. 21) disputed this hypothesis and argued that, in fact, the grain boundaries break away from solute atmospheres and leave them behind to form the "ghost" grain boundaries which are often observed in the HAZ of many alloys. As a result, they argued that the instantaneous solute concentration at the boundary reflects the concentration of the matrix through which it migrates. However, this model neglects two important considerations:

1. The potential for solute and/or interstitial atoms to be swept along with a moving boundary depends upon a number of factors including the relative diffusivity, boundary velocity, and affinity of the atomic species for surfaces and interfaces. As a result, it is possible that some solute and interstitial species are not capable of diffusing with a moving grain boundary and are left to form "ghost" HAZ boundaries. Other elements with high diffusivities may, in fact, be swept into and move with the boundary as the mobile grain boundary encounters regions which are enriched in this element.

2. The diffusivity along grain boundaries may be orders of magnitude greater than that of the bulk. Since grain boundaries are continuous across the fusion line, a continuous solute "pipeline" is established between the fusion zone and HAZ. Solute enrichment of fusion zone grain boundaries resulting from partitioning during solidification can then contribute to the solute concentration of HAZ grain boundaries.

Mechanism of HAZ Hot Cracking

Constitutional liquation of Ti-rich carbides can be observed immediately adjacent to the fusion line. However, it does not appear that this phenomenon contributes significantly to the onset of hot cracking. The observed grain boundary enrichment by titanium must, therefore, result from the accumulation of solute atoms along the grain boundary either by a "sweeping up" mechanism during the rapid grain growth stage of the HAZ thermal cycle, "pipeline" grain boundary diffusion from the fusion zone, or by a combination of these effects. Since titanium partitions to boundaries in the fusion zone during solidification (Ref. 22), titanium may migrate along the grain boundaries from the fusion zone into the HAZ. Additional titanium swept up during boundary migration serves to increase the solute concentration and slow the boundary motion by means of a solute drag effect.

Based on these hypotheses the model for HAZ hot cracking in alloy 800 can be summarized as follows:

1. During the on-heating portion of the weld thermal cycle MC and $M_{23}C_6$ carbides in the HAZ dissolve and allow rapid grain growth in the portion of the HAZ which experiences temperatures in the range from the solidus to approximately 1250°C (2282°F). Carbides immediately adjacent to the fusion line melt in situ by means of a constitutional liquation mechanism.

2. As the boundaries move, titanium from the dissolved carbides are swept up

and migrate with the boundary. The assimilated grain boundary titanium imposes a drag effect on the migration and effectively retards the grain growth in the region immediately adjacent to the fusion line.

3. Concurrently, titanium along fusion zone solidification boundaries may diffuse "downhill" along the boundary into the HAZ.

4. The titanium enrichment lowers the effective melting temperature of the boundary relative to the surrounding matrix and results in localized melting when the temperature exceeds approximately 1320°C (2408°F).

5. As the fusion zone solidifies or as the specimen is bent in the case of the Varestraint test, stress across the liquid boundary cannot be accommodated and a crack initiates.

6. As the crack opens under the imposed restraint liquid from the molten pool is drawn into the crack envelope by capillary action. The backfilling of the HAZ cracks by liquid from the fusion zone gives rise to the widened boundaries observed in Figs. 7-9.

It is likely that the silicon and phosphorus enrichment detected by the electron microprobe along HAZ boundaries (Fig. 9) results from the backfilling mechanism. In addition, titanium which has partitioned along fusion zone solidification boundaries and in advance of the solid-liquid interface contributes to the high concentration of this element and the formation of an M_2Ti phase along the backfilled boundary. The initial liquation of the HAZ boundary occurs prior to any backfilling from the fusion zone and results primarily from the grain boundary titanium enrichment described above.

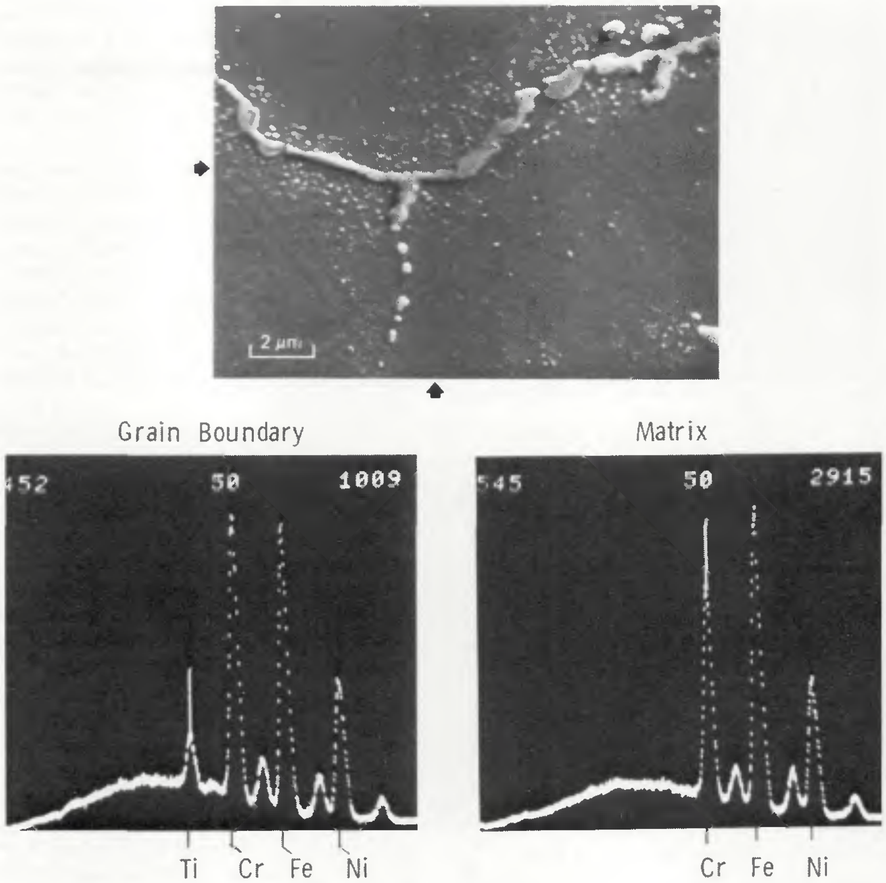

	G.B.	Matrix
Ti/Fe	0.30	<0.05
Cr/Fe	1.02	0.75
Ni/Fe	0.49	0.61

Fig. 15 — Carbide precipitation along HAZ grain boundaries following heat treatment at 1000°C (1832°F)

Table 3—Diffusivity of Ti, Cr, and C in Austenite

Element	Alloy system	Diffusivity, cm^2/s	Temperature, °C
Ti	Fe-Ti (Ref. 23)	3.8×10^{-11}	1000
		7.7×10^{-9}	1350
Cr	Fe-17Cr-12Ni (Ref. 24)	8.4×10^{-12}	1000
		1.2×10^{-9}	1350
C	Fe-15Cr-35Ni (Ref. 25)	8.5×10^{-7}	1000
		4.0×10^{-6}	1350

Postweld Sensitization

In order to map the titanium distribution in the HAZ following welding, a number of Varestraint specimens were heat treated at 1000°C (1832°F). This temperature corresponds to the nose of the TTP (time-temperature-precipitation) curve for titanium carbide (Ref. 7). Since titanium is concentrated along the HAZ boundaries during welding, the microstructure in this region is effectively "sensitized" by this heat treatment.

A SEM micrograph of the HAZ of a sensitized heat B specimen is shown in Fig. 15. Note that the carbide is continuous along the boundary and that discrete carbides are clustered in a band 2-3 µm wide on each side of the boundary. Results of chemical analysis of the boundary precipitate using the energy dispersive spectrometer (EDS) revealed a slight increase in chromium and decrease in nickel relative to the matrix, while the titanium concentration increased significantly over that of the matrix. The carbide network extended 3-4 grain diameters into the HAZ and was continuous across the fusion line along solidification boundaries in the fusion zone.

The extent of the grain boundary carbide network in the HAZ corresponds to the distance over which crack propagation was observed in the Varestraint samples. Beyond the crack susceptible region, carbides were observed to precipitate homogeneously both along austenite grain boundaries and within the grains.

The diffusivity of titanium, chromium, and carbon in austenite at 1350 and 1000°C (2462 and 1832°F) are listed in Table 3. Since the diffusivity of carbon is relatively high at 1000°C (1832°F), carbon is able to migrate rapidly through the matrix to sites where MC or $M_{23}C_6$ precipitates may form. Conversely, the diffusivity of both chromium and titanium is low; thus, these elements remain in nearly the same location that they occupied following welding.

Sensitization heat treatment obviously represents an effective means to map the titanium and, to a lesser degree, chromium distribution in the HAZ of alloy 800. It is clear from the microstructure in Fig. 15 that a large proportion of the titanium in the HAZ following welding is distributed along grain boundaries.

Effect of Solution Heat Treatment

The model for HAZ cracking requires

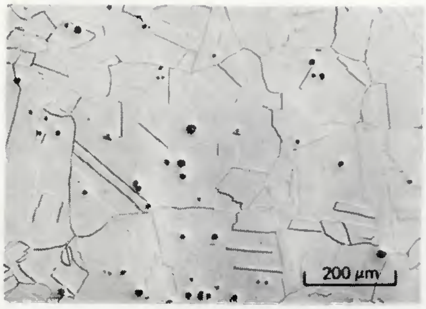

Fig. 16—Microstructure of a heat A Spot Varestraint sample solution annealed at 1150°C (2100°F) for 2 h, ×100 (reduced 50% on reproduction)

that titanium enrichment of grain boundaries occur by means of a simultaneous decomposition, grain growth, and solute sweeping mechanism. The rapid dissolution of Ti-rich carbides provides localized sites where titanium can be swept into the migrating boundaries. Based on this assumption an effort was made to improve the HAZ hot cracking resistance of alloy 800 by dissolving the small secondary carbides by means of a solution annealing heat treatment. As a result, grain boundary migration in the HAZ occurs within a homogeneous austenite matrix.

Spot Varestraint test bars of heat A, B, and D material were solution annealed at 1150°C (2100°F) for 2 hours (h). The resultant microstructure, shown in Fig. 16, exhibited a grain size of ASTM 3-4. The solution treated microstructures of these three heats were nearly identical to the as-received, solution annealed microstructure of heat C—Fig. 1.

Spot Varestraint test results of the solution treated (ST) samples are presented in bar graph form in Fig. 17. For comparison purposes, the as-received (AR) data at the same restraint level is included. In each case, the alloy in the solution treated condition exhibited less cracking than the same material in the mill-annealed condition.

The decrease in grain boundary area resulting from the solution heat treatment may have a slight effect on the results. However, measurements of grain size in the crack-sensitive region of the HAZ revealed that the final grain size in the HAZ of the solution treated samples was only slightly larger than that of the mill-annealed Varestraint specimens. This can be demonstrated by comparing the near-HAZ region of a solution treated heat A sample, shown in Fig. 18, with the as-received test specimen in Fig. 8. Despite the variation in heat treatment the morphology of the liquated HAZ boundaries appears similar.

It is evident from Fig. 17 that the cracking susceptibility of the four solution treated heats are nearly equivalent in contrast to the variation in crack susceptibility exhibited by the mill annealed microstructures. This observation strongly suggests that the presence of carbides in the base metal microstructure and the interaction of these carbides with mobile grain boundaries in the HAZ can influence the hot cracking susceptibility of alloy 800.

The similarity in crack susceptibility exhibited by the solution-annealed materials probably reflects the small difference in composition among the heats. The reduction in overall cracking relative to the mill-annealed (AR) microstructure reinforces the hypothesis that the dissolution of carbides in the HAZ provides Ti-rich sites where titanium can be swept into a grain boundary and depress the effective solidus temperature of the boundary region. In short, the Varestraint test results suggest that the HAZ hot cracking susceptibility of alloy 800 is influenced not only by the composition of the material but also by the form and distribution of the base metal carbides.

Summary

The Spot Varestraint test was employed to evaluate the heat-affected zone (HAZ) hot cracking susceptibility of five commercial heats of alloy 800. Although the heat-to-heat variation in crack susceptibility was relatively small, evaluation of individual samples revealed the underlying mechanism responsible for cracking in this alloy. Metallographic examination of the Varestraint samples revealed that HAZ hot cracks propagate along liquated boundaries in a region immediately adjacent to the fusion line. Microprobe analysis of the liquated boundaries revealed a 50-fold increase in titanium concentration relative to the bulk composition.

A mechanism has been proposed to explain the grain boundary liquation which gives rise to hot cracking in alloy 800. During the on-heating portion of the thermal excursion in the HAZ, MC and $M_{23}C_6$ carbides (carbonitrides) rapidly dissolve and permit grain growth to occur. As the grain boundaries migrate, they encounter Ti-rich sites previously occupied by MC-type precipitates. Titanium from these sites is swept into the boundary and diffuses with the boundary as grain growth continues. The localized titanium enrichment lowers the effective melting temperature of the boundary and results in grain boundary liquation in regions of the HAZ heated above approximately 1320°C (2408°F). If sufficient restraint is present, these boundaries become preferential sites for hot crack formation.

The form and distribution of the carbides in the initial base metal microstructure can have a pronounced effect on the susceptibility of the alloy to HAZ hot cracking. Alloys, which were mill-annealed and exhibited a biomodal distribution of carbides, were found to be more crack susceptible than the same alloy composition which was solution-annealed and exhibited only the large, stable MC-type carbides. The absence of the small MC and $M_{23}C_6$ carbides (carbonitrides) in the solution-annealed microstructure mitigates the grain bound-

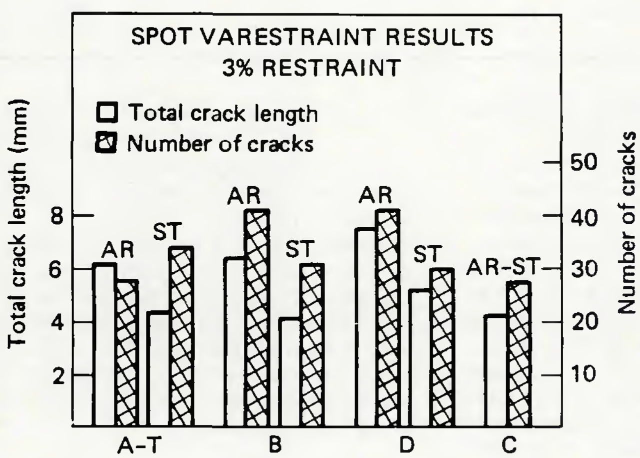

Fig. 17—Results of Spot Varestraint tests of as-received (AR) and solution treated (ST) microstructures of heats A, B, and D at 3% restraint

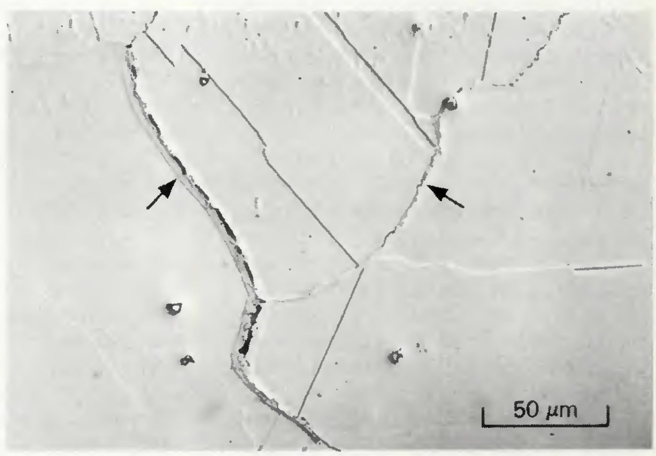

Fig. 18—Liquated HAZ grain boundary in a solution treated Spot Varestraint sample from heat A tested at 3% restraint, ×400 (reduced 31% on reproduction)

ary sweeping effect and thus reduces the hot cracking susceptibility.

Attempts by previous investigators (Ref. 1-3) to relate the HAZ hot cracking susceptibility of alloy 800 to specific heat-to-heat chemistry variations have been largely unsuccessful due to the important influence of heat-to-heat variations in microstructure. The results of this investigation have shown that careful control of base metal microstructure — in particular, the nature and distribution of carbides — is essential in order to ensure adequate resistance to HAZ hot cracking in alloy 800 weldments.

Acknowledgments

The author wishes to thank W. B. Jones of the Sandia National Laboratories in Albuquerque, N.M., for providing the material which was evaluated in this investigation. The welding and metallographic support of R. A. Bell, the microanalysis performed by R. E. Gorniak and C. W. Karfs, and the Auger analysis performed by W. M. Clift, all of this laboratory, are greatly appreciated. This work was supported by the U. S. Department of Energy under contract number DE-AC04-75DP00789.

References

1. Canonico, D. A., Savage, W. F., Werner, W. J., and Goodwin, G. M. 1969. Effects of minor additions on weldability of Incoloy 800. *Effects of minor elements on the weldability of high-nickel alloys (proceedings of symposium),* pp. 68-92. New York: The Welding Research Council.

2. King, J. F., and Reed, R. W., Jr. 1976 (April). *Weldability testing of Alloy 800.* ORNL Report No. TM-6276.

3. York, J. W., and Flury, R. L. 1976 (Feb). *Assessment of candidate weld metals for joining alloy 800.* Westinghouse Electric Corp., Tampa Division, Report No. WNET-119.

4. Goodwin, G. M., Savage, W. F., and Nippes, E. F. 1977. Effects of minor elements on hot-cracking tendencies of Inconel 600. *Welding Journal* 56(8):238-s to 244-s.

5. Casteras, J. E., Savage, W. F., and Nippes, E. F. 1978. Effect of alloying additions on the weldability of 70Cu-30Ni. *Welding Journal* 57(12):375-s to 382-s.

6. Turner, P. W., and Lundin, C. D. 1970. Effect of iron on the hot cracking of uranium weld metal — part 1. *Welding Journal* 49(12):579-s to 587-s.

7. Allen, R. M., and Jones, W. B. 1982. Mechanical Behavior of Alloy 800 at 838 K. *Met. Trans.* 13A(4):637-648.

8. Arata, Y., Matsuda, F., and Katayama, S. Solidification crack susceptibility in weld metals of fully austenitic stainless steels (report II) — effect of ferrite, P, S, C, Si, and Mn on ductility properties of solidification brittleness. *JWRI Trans.* 6(1):105-116.

9. Miller, T. W., Savage, W. F., and Nippes, E. F. 1976. Microsegregation in 70Cu-30Ni weld metal. *Welding Journal* 55(6):181-s to 188-s.

10. Lippold, J. C. 1981. Unpublished research.

11. Brooks, J. A. 1974. Effect of alloy modifications on HAZ cracking of A-286 stainless steel. *Welding Journal* 53(11):517-s to 523-s.

12. *Metals Handbook*, vol. 8, p. 307. Metals Park, Ohio: American Society for Metals.

13. Pepe, J. J., and Savage, W. F. 1967. Effects of constitutional liquation in 18-Ni maraging steel weldments. *Welding Journal* 46(a):411-s to 422-s.

14. Pepe, J. J., and Savage, W. F. 1970. The weld heat-affected zone of the 18-Ni maraging steels. *Welding Journal* 49(12):545-s to 553-s.

15. Savage, W. F., and Krantz, B. M. 1966. An investigation of hot cracking in Hastelloy X. *Welding Journal* 31(1):13-s to 25-s.

16. Owczarski, W. A., Duvall, D. S., and Sullivan, C. P. 1966. A model for heat-affected zone cracking in nickel-base superalloy. *Welding Journal* 45(4):145-s to 155-s.

17. Duvall, D. S., and Owczarski, W. A. 1967. Further heat-affected zone studies in heat-resistant nickel alloys. *Welding Journal* 46(9):423-s to 432-s.

18. Vinckier, A. G. 1971. Micro-hot tearing in the heat-affected zone of high strength steels. *Welding Journal* 50(1):19-s to 24-s.

19. Tamura, H., Katayama, N., and Watanabe, T. 1974. Hot cracking in synthetic weld heat-affected zone Ni-Cr-Mo-type higher strength steel. *Trans. JWS* 5(2):72-82.

20. Robinson, J. L., and Scott, M. H. 1980. Liquation cracking during the welding of austenitic stainless steels and nickel alloys. *Phil. Trans. R. Soc. Lond. A 295,* pp. 105-117.

21. Duvall, D. S., and Owczarski, W. A. 1966. Technical note: behavior of solute at mobile heat-affected zone grain boundaries. *Welding Journal* 45(8):356-s.

22. Unpublished research performed at Sandia Laboratories, Livermore, California, 1981.

23. Swisher, J. H. 1968. Sulfur solubility and internal sulfidation of iron-titanium alloys. *Met. Trans., vol. 242,* pp. 2433-2439.

24. Perkins, R. A., Padgett, R. A., and Tunala, N. K. 1973. Tracer diffusion of 59 Fe and 51 Cr in Fe-17Cr-12Ni austenitic alloy. *Met. Trans.* 4(11):2535-2540.

25. Demel, O. 1977. *Radek Rundsch,* (2), pp. 201-209.